ChemPubSoc Europe

DOI: 10.1002/open.201800294

Open Access ChemistryOPEN Communications

Monitoring Hydrogenation Reactions using Benchtop 2D NMR with Extraordinary Sensitivity and Spectral Resolution

Dariusz Gołowicz,[a, b] Krzysztof Kazimierczuk,*[b] Mateusz Urbańczyk,[b, c] and Tomasz Ratajczyk*[d]

Low-field benchtop nuclear magnetic resonance (BT-NMR) spectrometers with Halbach magnets are being increasingly used in science and industry as cost-efficient tools for the monitoring of chemical reactions, including hydrogenation. However, their use of low-field magnets limits both resolution and sensitivity. In this paper, we show that it is possible to alleviate these two problems through the combination of parahydrogen-induced polarization (PHIP) and fast correlation spectroscopy with time-resolved non-uniform sampling (TR-NUS). PHIP can enhance NMR signals so that substrates are easily detectable on BT-NMR spectrometers. The interleaved acquisition of one- and two-dimensional spectra with TR-NUS provides unique insight into the consecutive moments of hydrogenation reactions, with a spectral resolution unachievable in a standard approach. We illustrate the potential of the technique with two examples: the hydrogenation of ethylphenyl propiolate and the hydrogenation of a mixture of two substrates – ethylphenyl propiolate and ethyl 2-butynoate.

High-field nuclear magnetic resonance (NMR) offers a variety of powerful analytical techniques that provide qualitative and quantitative information about samples in a comprehensive and a non-destructive way. Unfortunately, purchasing and maintaining high-field NMR instruments is expensive. One possible solution is to use low-field benchtop NMR (BT-NMR) spectrometers with low-cost Halbach permanent magnets. Besides having low handling costs, BT-NMR instruments are highly portable and can easily be connected to a variety of chemical reactors.[1] However, despite many technological improvements, BT-NMR spectrometers still suffer from poor resolution and low sensitivity. This is due to the relatively low magnetic field strength provided by their permanent magnets. Enhancing the NMR signal is therefore of crucial importance for the wider application of BT-NMR. This is possible by means of various hyperpolarization techniques, in particular employing parahydrogen, which greatly enhances the NMR signal in an inexpensive and convenient manner.[2,3] The idea behind this approach is to exploit the unique properties of hydrogen molecules, which can exist in the form of two spin isomers: orthohydrogen (o-H_2) and parahydrogen (p-H_2).[4] At room temperature the hydrogen gas contains approximately 25% p-H_2 and 75% o-H_2. As the temperature falls, o-H_2 is converted into p-H_2 and the hydrogen gas mixture becomes gradually enriched in p-H_2. For such an interchange to take place, we need a suitable catalyst, such as charcoal.[5] Parahydrogen-enriched gas, usually referred to as simply "parahydrogen", has very interesting properties with regard to NMR signal enhancement: It is a reservoir of high nuclear spin polarization that can be transferred to other molecules in order to enhance their NMR signals by up to a few orders of magnitude. The enhancement under discussion can be obtained through reversible interaction (SABRE – Signal Amplification by Reversible Exchange)[6] or by hydrogenation with p-H_2 (PHIP – Parahydrogen Induced Polarization).[7] The latter method is an excellent way to monitor hydrogenation reactions, which are among the most important chemical reactions in industry and research.[8] Indeed, one-dimensional (1D) NMR with PHIP, on both low-field BT and high-field spectrometers, has already been demonstrated for the monitoring of hydrogenation processes for homogeneous and heterogeneous systems.[9] PHIP can be also utilized for observation of hydrogenation processes on TD analyzers.[10] However, in principle, 1D NMR is less informative than the two-dimensional (2D) NMR technique. For this reason, a combination of 1D and 2D reaction monitoring at the same time is desirable. This can be achieved by means of time-resolved non-uniform sampling (TR-NUS) of a 2D signal interleaved with 1D acquisition. The concept of TR-NUS has been demonstrated in several different applications, ranging from following biochemical reactions[11] to monitoring molecular structure changes with temperature[12] or metabolism *in vivo*.[13] Figure 1 shows the concept underlying the TR-NUS

[a] *D. Gołowicz*
Faculty of Chemistry, Biological and Chemical Research Centre
University of Warsaw
Żwirki i Wigury 101, 02-089 Warsaw (Poland)
[b] *D. Gołowicz, Dr. K. Kazimierczuk, Dr. M. Urbańczyk*
Centre of New Technologies
University of Warsaw
Banacha 2 C, 02-097 Warsaw (Poland)
E-mail: k.kazimierczuk@cent.uw.edu.pl
[c] *Dr. M. Urbańczyk*
NMR Research Unit
University of Oulu
90014 Oulu (Finland)
[d] *Dr. T. Ratajczyk*
Institute of Physical Chemistry
Polish Academy of Sciences
Kasprzaka 44/52, 01-224 Warsaw (Poland)
E-mail: tratajczyk@ichf.edu.pl

Supporting information for this article is available on the WWW under https://doi.org/10.1002/open.201800294

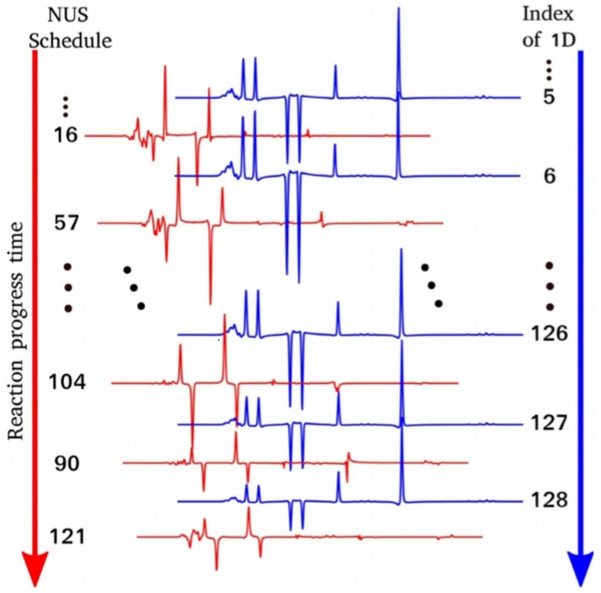

Figure 1. The concept of TR-NUS with interleaved acquisition of 1D spectra, using data from current study. Blue spectra correspond to interleaved ^{1}H NMR experiments, whereas red spectra correspond to increments of NUS DQF-COSY spectra (acquired in accordance to the NUS Schedule). Acquisition is performed in parallel to the reaction.

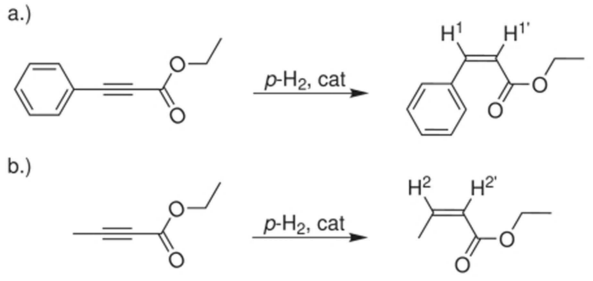

Figure 2. Hydrogenation reactions used in this study.

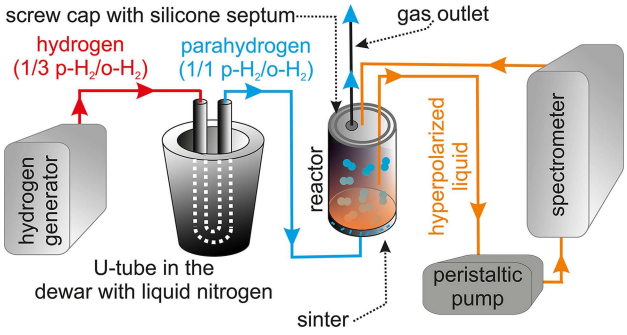

Figure 3. Experimental setup for monitoring hydrogenation reactions.

approach. A shuffled non-uniform sampling is performed in parallel to the process occurring in the NMR tube. As shown, the sampling of the indirect evolution time in the NMR experiment can be interleaved with measurements of 1D FIDs. 2D spectra are reconstructed from consecutive, overlapping subsets of the data, forming a pseudo-3D object that shows the changes of the spectrum caused by the process being monitored.

It is possible to reconstruct the TR-NUS signal with any of the NUS methods used in NMR, applied to each of the subsets separately.[14,15] One method that has become very popular over the past decade is "compressed sensing" (CS).[11,12,13,16] CS is based on the assumption, that spectrum is sparse ("almost empty")[17] and thus can be recovered from small fraction of the data required by Fourier Transform (FT). Importantly for the current study, rapid changes of signal amplitude within the subset result in undesired t_1-noise artifacts and should be minimized.[18]

In this study we demonstrate that the low resolution and sensitivity limitations of BT-NMR spectrometers can be alleviated by simultaneously implementing PHIP and TR-NUS. In particular, we show that a novel combination of PHIP and TR-NUS on benchtop spectrometers is an excellent tool for monitoring hydrogenation reactions.

We tested the method using two kinds of samples: a single-component mixture and a two-component mixture. In the first case, we monitored the hydrogenation of ethylphenyl propiolate to (Z)-ethyl cinnamate (Figure 2a). In the second, we also monitored the hydrogenation of ethyl 2-butynoate to (Z)-ethyl crotonate (Figure 2b).

We performed all our experiments on a Magritek Carbon 43 MHz benchtop spectrometer equipped with a flow cell. We slowly bubbled gaseous hydrogen enriched with a *para*-state isomer (approximately 50 %) through a flask placed outside the magnet (in the Earth's magnetic field). The mixture was continuously pumped through a spectrometer in a closed circuit (Figure 3).

In both examples we employed the same TR-NUS procedure, with the interleaved acquisition[19,20] of a 2D double-quantum filtered correlation spectroscopy (NUS DQF-COSY) and 1D proton spectrum. The 1D spectra of the first reaction (Figure 2a) reveal that amplified signals of peaks H^1 and $H^{1'}$ reach their maximum shortly after the hydrogen gas flow is turned on (Figure 4). The delay is caused by the time required for saturation of a liquid with p-H_2. During the reaction, the

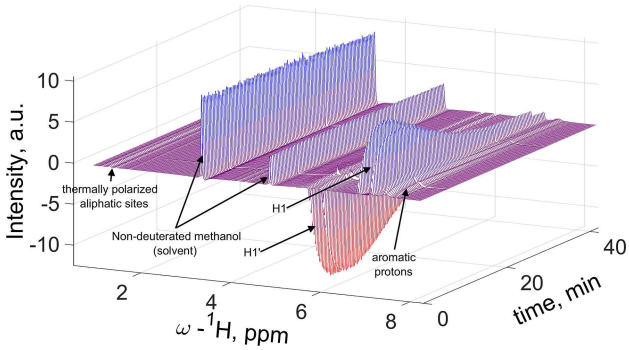

Figure 4. Stack of acquired ^{1}H NMR spectra in an interleaved manner showing peak intensity changes during the course of the reaction from Figure 2a. Enhanced peaks H^1 and $H^{1'}$ show characteristic rapid growth at the beginning and exponential decay after crossing the maximum. The multiplet pattern is typical for adiabatic longitudinal transport after dissociation engenders net alignment (ALTADENA) conditions for PHIP.

signals of the hyperpolarized product decay, as their intensity depends on the rate of p-H_2 addition. The decay curves for the protons H^1 and $H^{1'}$ are smooth, which indicates adequate stability of our simple home-built apparatus (Figures 4 and 5) and is of particular importance for the acquisition of 2D data. We observe an up to 600-fold enhancement of the signal intensity in 1D experiments. We also see some enhancement of the signals of the aromatic protons due to the isotropic mixing polarization transfer mechanism.[21]

Reaction tracking with 2D NMR provides increased spectral resolution and reveals more structural details. Although, in the first example, the enhanced peaks were already well separated in the ^{1}H spectrum, we measured a series of interleaved TR-NUS DQF-COSY to demonstrate that they preserve the same temporal information as a series of ^{1}H NMR (see Figure 5). A decay curve extracted from TR-NUS DQF-COSY fits very well into the 1D NMR curve. We observed only a slight temporal inconsistency caused by signal averaging within a data subset in TR-NUS. For fast changing signals, like in our example of the hydrogenation, the subset size should be as small as possible, enabling proper reconstruction of a 2D spectrum and providing acceptable signal averaging.[12,18] TR-NUS DQF-COSY also provides better resolution and shows the connectivity of atoms.

The increased resolution provided by 2D experiments is even clearer in the second example, where we studied a mixture of two substrates. In contrast to the hyperpolarized (Z)-ethyl cinnamate product, the (Z)-ethyl crotonate molecule possesses distinctive three-bond J-coupling between attached

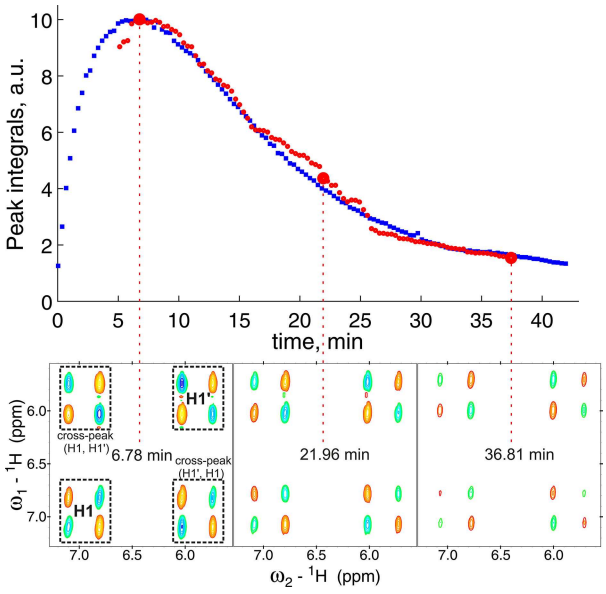

Figure 5. Results of monitoring the reaction from Figure 2a. Integrals of enhanced H^1 and $H^{1'}$ signals in both ^{1}H NMR and 2D NUS DQF-COSY spectra (upper plot). Integrals obtained from ^{1}H NMR spectra are marked blue, whereas points corresponding to integrals of the enhanced cross peaks in NUS DQF-COSY spectra are marked red. Three selected 2D spectra (bottom plots) show decaying cross peaks during the course of the hydrogenation reaction. The temporal resolution of the interleaved 2D and 1D spectra was 19.8 seconds, and the reaction was monitored for 42 minutes. The interleaved TR-NUS experiment resulted in 128 ^{1}H NMR and 96 NUS DQF-COSY spectra.

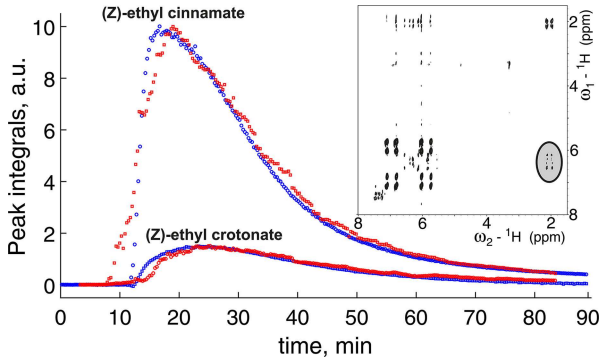

Figure 6. Integrals of enhanced signals in ^{1}H NMR (blue) and 2D NUS-DQF COSY spectra (red) during the hydrogenation reactions of a mixture of two substrates. The inset spectrum presents a selected frame of the 2D NUS-DQF COSY. This time, signal acquisition began about 12 minutes before turning on the gas flow. We observed a stronger signal enhancement for (Z)-ethyl cinnamate (Figure 2a). The two substrates reached maximum intensity at slightly different time points: (Z)-ethyl cinnamate at 18.03 minutes and (Z)-ethyl crotonate at 24.33 minutes. The temporal resolution of the interleaved 2D and 1D spectra was 18 seconds, and total experimental time 90 minutes. The results shown are for 300 ^{1}H NMR spectra and 268 2D NUS DQF-COSY acquired in an interleaved manner. The distinctive cross peak for (Z)-ethyl crotonate is marked with a gray ellipse.

hydrogen atom and adjacent methyl hydrogens. This leads to the transfer of non-Boltzmann polarization through a 2D pulse sequence between coupled nuclei, giving rise to enhanced, well-separated cross peaks in NUS-DQF COSY spectra (Figure 6). Using the comparison of the reaction progress curves for the two products, extracted from interleaved 1Ds or 2Ds, it would be possible to investigate the kinetics of parallel reactions and explore the properties of a catalyst in a mixture of substrates.

As mentioned above, although changes in signal intensity encode the reaction progress, they disturb the quality of reconstructed 2D spectra. This is due to the t_1-noise artifacts that arise from the change in signal intensity within a data subset used for a single 2D spectrum reconstruction.[18] The resulting artifacts may also bury some of the weak cross-peaks present in a spectrum and therefore introduce ambiguities into the assignment. Note that rapid signal enhancement at the initial stage of PHIP hydrogenation causes an extreme amplitude variation and leads to substantial t_1-noise artifacts. However, a simple solution is possible during post-processing by taking advantage of interleaved 1D experiments. We can reduce the amplitude variation of the enhanced signals in the t_1 dimension to some extent by selectively weighting enhanced regions in non-reconstructed data. We obtained a proper weighting function by fitting a polynomial to the reaction progress curve obtained from the interleaved 1D spectra. We have demonstrated t_1-noise artifact correction procedures (Figure 7) on data acquired for hydrogenation of a single substrate (Figure 2a). The selective weighting procedure can be optionally applied in a post-processing stage to increase readability of spectra or if a single high quality enhanced 2D spectrum is desired. If it is applied to the whole dataset together (as in this study), the effect of the reaction progress is not visible in the spectra anymore. Alternatively, one could apply the same procedure within each frame separately, to preserve the effect.

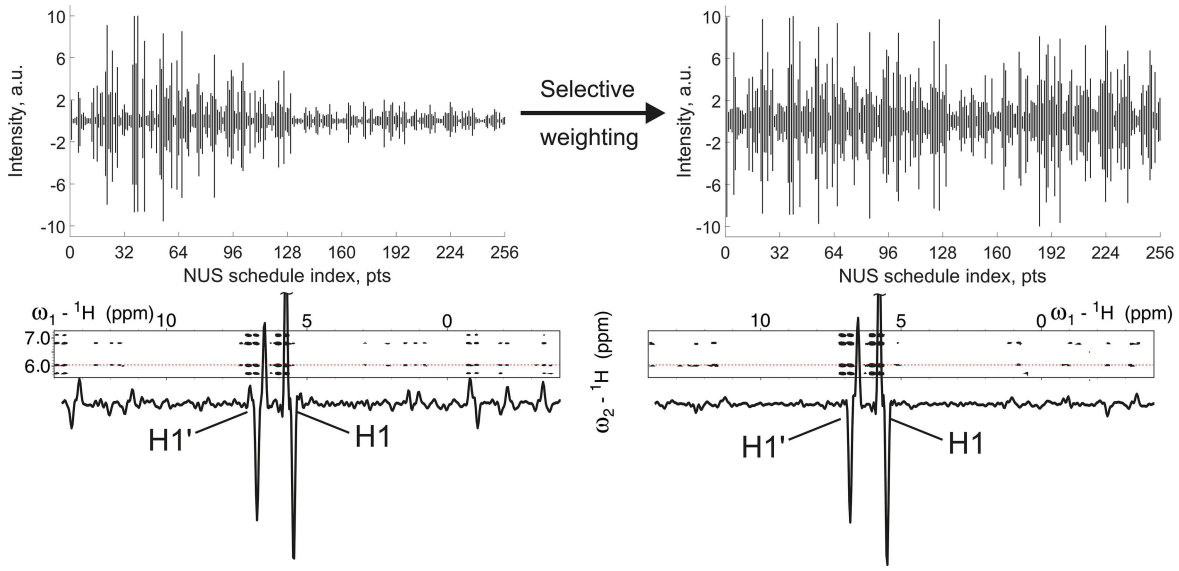

Figure 7. Non-uniformly sampled points of the t_1 dimension before (upper left) and after (upper right) application of selective weighting. Both upper plots are 2D NUS FID signals viewed from the perspective of the NUS t_1 domain. Instead of 128 points, there are 256 points, as every second point stands for a States quadrature. Signal intensities reflect the enhancement profile (see Figure 5) and are flattened after selective weighting. NUS DQF-COSY spectra (bottom plots) were obtained from both datasets using 64 NUS points (half of a full dataset), while the maximum increment in a spectrum was 128. The spectrum reconstructed from the original dataset (bottom left) suffers from significant NUS t_1-noise artifacts, while the spectrum reconstructed from the weighted dataset (bottom right) is much less noisy.

The non-stationary nature of enhanced signals in PHIP hinders conventional acquisition of 2D spectrum. In this area, other possible solutions have been already reported, including ultrafast NMR or extended para-hydrogenation method.[22]

In summary, in this article we report for the first time on the PHIP technique, combined with TR-NUS. We implemented both of these powerful methods on BT-NMR spectrometers, which are increasingly popular today. We consider this method as a valuable tool for monitoring hydrogenation reactions, as it enables measurement beyond the standard limit of detection and resolution provided by the commonly employed 1D NMR. We also show how the interleaved acquisition of 1D and 2D data can help to reduce t_1-noise artifacts in the 2D NUS spectrum. We believe that the approach presented here has the potential to be applied as a cost-efficient and convenient tool in scientific and industrial laboratories.

Experimental Section

Experimental Setup

Figure 3 shows the experimental setup in schematic form. As the source of hydrogen (75% o-H_2, 25% p-H_2), we employed a hydrogen generator, model HYGEN3000. The hydrogen gas was enriched up to 50% in a p-H_2 at a liquid nitrogen temperature over activated charcoal (granulates 1–4 mm) in a U-tube. The reactor was specially built for us by a glassblower. Parahydrogen gas was administered through the sinter, which was on the bottom of the reactor. The sinter ensured uniform bubbling of the parahydrogen throughout the liquid. The reactor had a screwcap with a septum on the top, through which three hoses were passed. Two hoses were connected to the peristaltic pump, which pumped the liquid to the measurement cell in the BT-NMR spectrometer. The third hose was for parahydrogen gas release – experiments were performed under atmospheric pressure. The end of the hose that was for drawing liquid from the reactor to the spectrometer was equipped with a protective cap that prevented bubbling gas from getting into the hose, and consequently into the BT-NMR spectrometer cell.

Solution for Hyperpolarization

We made a single-component substrate solution by mixing 2 ml of ethylphenyl propiolate (Merck) with 14 ml of methanol (Linegal Chemicals) and dissolving 5.5 mg of **[Rh(dppb)(COD)]BF4** catalyst (Merck) in it. We used the same quantities of chemicals to prepare a second sample (mixture) with an extra 2 ml of a second substrate – ethyl 2-butynoate (Merck).

Hydrogenation Monitoring

We injected the reaction mixture through the septum into the reactor. The peristaltic pump was started with a flow speed of 3.45 mL/min, and after approximately 60 seconds, when everything was stable, a lock signal was found. Following this, we pumped parahydrogen gas into the reactor and monitored the hydrogenation reaction.

Acquisition and Processing

In our interleaved PHIP TR-NUS measurements, every acquired ^1H spectrum was followed by the acquisition of the t_1 point of the DQF-COSY experiment. We grouped together the acquired t_1 points and then divided them into overlapping subsets. Next, we reconstructed each subset separately using 30 iterations of a Compressed-Sensing-based Iterative Reweighted Least Squares algorithm (CS-IRLS).[14] The algorithms used for the reconstruction are freely available in mddNMR software.[23] Convenient TR-NUS

setup and processing is possible using TReNDS software.[20] The interleaved 1D experiment was the 0th increment of DQF-COSY, which is the equivalent of ^{1}H NMR acquired with a 270-degree pulse. 1D and 2D spectra were recorded with 1 scan and 4 scans per increment. For the first example studied we acquired 128 NUS points, and for the second 300 NUS points, while the maximum allowed increment in the NUS schedule was 128 for both. For the single spectrum reconstruction we used 32 NUS points (25 percent of a full grid). The repetition time between each scan was 2.2 seconds for the first example and 2.0 seconds for the second example. The chemical shift scale in all experiments was referenced to the peak of methanol at 3.34 ppm. We modified the DQF-COSY pulse sequence available in the Magritek Spinsolve Expert operating software to work in a States quadrature mode.[24] We performed seventh-order polynomial fitting of a signal enhancement curve, selective weighting of 2D data for t_1-noise artifacts reduction and integration of 1D and 2D peaks in a MATLAB R2013b. The description of a pulse sequence, macro for acquisition and code for selective weighting can be found in ESI.

Acknowledgements

The authors would like to thank the National Science Centre of Poland for support us with the grants OPUS 11 (2016/21/B/ST4/02162) and OPUS 9 (2015/17/B/ST4/04221). MU acknowledges financial support from the Kvantum Institute (University of Oulu).

Conflict of Interest

The authors declare no conflict of interest.

Keywords: parahydrogen-induced polarization · benchtop NMR · non-uniform sampling · reaction monitoring

[1] a) F. Dalitz, M. Cudaj, M. Maiwald, G. Guthausen, *Prog. Nuc. Mag. Res. Spec.* **2012**, *60*, 52–70; b) B. Bluemich, K. Singh, *Angew. Chem. Int. Ed.* **2018**, *57*, 6996–7010; *Angew. Chem.* **2018**, *130*, 7114–7129; c) S. S. Zalesskiy, E. Danieli, B. Bluemich, V. P. Ananikov, *Chem. Rev.* **2014**, *114*, 5641–5694.

[2] M. E. Halse, *TrAC Trends Anal. Chem.* **2016**, *83*, 76–83

[3] K. V. Kovtunov, E. V. Pokochueva, O. G. Salnikov, S. Cousin, D. Kurzbach, B. Vuichoud, S. Jannin, E. Y. Chekmenev, B. M. Goodson, D. A. Barskiy, I. V. Koptyug, *Chem. Asian J.* **2018**, *13*, 1857–1871.

[4] A. Farkas, Orthohydrogen, *Parahydrogen and Heavy Hydrogen*, Cambridge University Press, Cambridge, **1935**.

[5] G. Buntkowsky, B. Walaszek, A. Adamczyk, Y. Xu, H. H. Limbach, B. Chaudret, *Phys. Chem. Chem. Phys.* **2006**, *8*, 1929–1935.

[6] a) R. W. Adams, J. A. Aguilar, K. D. Atkinson, M. J. Cowley, P. I. P. Elliott, S. B. Duckett, G. G. R. Green, I. G. Khazal, J. Lopez-Serrano, D. C. Williamson, *Science* **2009**, *323*, 1708–1711; b) M. J. Cowley, R. W. Adams, K. D. Atkinson, M. C. R. Cockett, S. B. Duckett, G. G. R. Green, J. A. B. Lohman, R. Kerssebaum, D. Kilgour, R. E. Mewis, *J. Am. Chem. Soc.* **2011**, *133*, 6134–6137; c) P. J. Rayner, S. B. Duckett, *Angew. Chem. Int. Ed.* **2018**, *57*, 6742–6753; *Angew. Chem.* **2018**, *130*, 6854–6866.

[7] a) C. R. Bowers, D. P. Weitekamp, *J. Am. Chem. Soc.* **1987**, *109*, 5541–5542; b) C. R. Bowers, D. P. Weitekamp, *Phys. Rev. Lett.* **1986**, *57*, 2645–2648; c) T. C. Eisenschmid, R. U. Kirss, P. P. Deutsch, S. I. Hommeltoft, R. Eisenberg, J. Bargon, R. G. Lawler, A. L. Balch, *J. Am. Chem. Soc.* **1987**, *109*, 8089–8091; d) M. G. Pravica, D. P. Weitekamp, *Chem. Phys. Lett.* **1988**, *145*, 255–258; e) R. A. Green, R. W. Adams, S. B. Duckett, R. E. Mewis, D. C. Williamson, G. G. R. Green , *Progress Nucl. Magn. Reson. Spectrosc.* **2012**, *67*, 1–48.

[8] a) K. V. Kovtunov, O. G. Salnikov, V. V Zhivonitko, I. V. Skovpin, V. I. Bukhtiyarov, I. V. Koptyug, *Top. Catal.*, **2016**, *59*, 1686–1699; b) S. Abdulhussain, H. Breitzke, T. Ratajczyk, A. Grunberg, M. Srour, D. Arnaut, H. Weidler, U. Kunz, H. J. Kleebe, U. Bommerich, J. Bernarding, T. Gutmann, G. Buntkowsky, *Chem. Eur. J.* **2014**, *20*, 1159–1166.

[9] a) K. Jeong, S. Min, H. Chae, S. K. Namgoong, *Magn. Reson. Chem.* **2018**, *56*, 1089–1093; b) K. Jeong, S. Min, H. Chae, S. K. Namgoong, *Magn. Reson. Chem.* **2019**, *57*, 44–48; c) D. B. Burueva, L. M. Kovtunova, V. I. Bukhtiyarov, K. V. Kovtunov, I. V. Koptyug, *Chem. Eur. J.* **2018**, *24*, 1–1; d) K. V. Kovtunov, L. M. Kovtunova, M. E. Gemeinhardt, A. V. Bukhtiyarov, J. Gesiorski, V. I. Bukhtiyarov, E. Y. Chekmenev, I. V. Koptyug, B. M. Goodson, *Angew. Chem. Int. Ed.* **2017**, *56*, 10433–10437; *Angew. Chem.* **2017**, *129*, 10569–10573; e) D. A. Barskiy, O. G. Salnikov, R. V. Shchepin, M. A. Feldman, A. M. Coffey, K. V. Kovtunov, I. V. Koptyug, E. Y. Chekmenev, *J. Phys. Chem. C* **2016**, *120*, 29098–29106.

[10] a) T. Ratajczyk, T. Gutmann, S. Dillenberger, S. Abdulhussaein, J. Frydel, H. Breitzke, U. Bommerich, T. Trantzschel, J. Bernarding, P. C. M. M. Magusin, G. Buntkowsky, *Solid State Nucl. Magn. Reson.* **2012**, *43–44*, 14–21; b) I. Prina, L. Buljubasich, R. H. Acosta, *J. Magn. Reson.* **2015**, *251*, 1–7

[11] M. Mayzel, J. Rosenlöw, I. Linnéa, V. Y. Orekhov, *J. Biomol. NMR.* **2014**, *58*, 129–139

[12] W. Bermel, R. Dass, K. P. Neidig, K. Kazimierczuk, *ChemPhysChem* **2014**, *15*, 2217–2220

[13] a) R. Dass, K. Grudziąż, T. Ishikawa, M. Nowakowski, R. Dębowska, K. Kazimierczuk, *Front. Microbiol.* **2017**, *8*, 1–12; b) R. Dass, W. Koźmiński, K. Kazimierczuk, *Anal. Chem.* **2015**, *87*, 1337–1343

[14] a) K. Kazimierczuk, V. Y. Orekhov, *Angew. Chem. Int. Ed.* **2011**, *50*, 5556–5559

[15] a) D. J. Holland, M. J. Bostock, L. F. Gladden, D. Nietlispach, *Angew. Chem. Int. Ed. Engl.* **2011**, *50*, 6548–6551 b) J. C. J. Barna, S. M. Tan, E. D. Lade. *J. Magn. Reson.* **1988**, 78, 327–332; c) B. E. Coggins, P. Zhou, *J. Biomol. NMR.* **2008**, *42*, 225–239; d) J. Stanek, W. Koźmiński, *J. Biomol. NMR.* **2010**, *47*, 65–77; e) J. Ying, F. Delaglio, D. A. Torchia, A. Bax, *J. Biomol. NMR.* **2017**, *68*, 101–118; f) M. Mobli, J. C. Hoch. *Concepts Magn. Reson. Part A* **2008**, *32A*, 436–448; g) S. G. Hyberts, D. P. Frueh, H. Arthanari, G. Wagner, *J. Biomol. NMR.* **2009**, *45*, 283–294; h) Y. Matsuki, M. T. Eddy, J. Herzfeld, *J. Am. Chem. Soc.* **2009**, *131*, 4648–4656

[16] Y. Wu, C. D'Agostino, D. Holland, L. F. Gladden, *Chem. Commun.* **2014**, *50*, 14137–14140

[17] a) E. J. Candes, M. B. Wakin, *IEEE Sig. Proc. Mag.* **2008**, *25*, 21–30; b) A. Shchukina, P. Kasprzak, R. Dass, M. Nowakowski, K. Kazimierczuk, *J. Biomol. NMR.* **2017**, *68*, 79–98.

[18] R. Dass, P. Kasprzak, W. Koźmiński, K. Kazimierczuk, *J. Magn. Reson.* **2016**, *265*, 108–116

[19] V. A. Jaravine, A. V. Zhuravleva, P. Permi, I. Ibraghimov, V. Y. Orekhov, *J. Am. Chem. Soc.* **2008**, *130*, 3927–3936

[20] M. Urbańczyk, A. Shchukina, D. Gołowicz, K. Kazimierczuk, *Magn. Reson. Chem.* **2019**, *57*, 4–12

[21] J. Natterer, J. Bargon, *Prog. Nuc. Mag. Res. Spec.* **1997**, *31*, 293–315

[22] a) S. Ahola, V. V. Zhivonitko, O. Mankinen, G. Zhang, A. M. Kantola, H. Chen, C. Hilty, I. V. Koptyug, V.-V. Telkki, *Nat. Commun.* **2015**, *6*, 8363; b) J. A. Tang, F. Gruppi, R. Fleysher, D. K. Sodickson, J. W. Canary, A. Jerschow, *Chem. Commun.* **2010**, *47*, 958–960

[23] V. Y. Orekhov, V. Jaravine, M. Mayzel, K. Kazimierczuk, mddnmr.spektrino.com, **2004–2018**.

[24] D. J. States, R. A. Haberkorn, D. J. Ruben, *J. Magn. Reson.* **1982**, *48*, 286–292

Manuscript received: December 27, 2018
Revised manuscript received: January 21, 2019